



**FACULTY OF CIVIL
ENGINEERING
CTU IN PRAGUE**

Czech Technical University in Prague
Faculty of Civil Engineering
Department of Mechanics
Thákurova 7, 166 29, Praha 6

MALCoLM

Multi-spiral column simulation module

Version 1.0

Software documentation of OOFEM extension module

TAČR-MOST Project CeSTaR: Computer simulation and experimental validation -
complex service for flexible and efficient design of pre-cast concrete columns with
innovative multi-spiral reinforcement

Author: P. Havlásek

December 2019

Report No. TF05000040-2019V002

Contents

1	Introduction and general information	3
1.1	Multi-spiral reinforcement	3
2	Computational model	6
3	Material models	7
3.1	CDPM2	7
3.1.1	Estimation of physically-based material parameters	7
3.2	Plasticity model for reinforcement	9
4	Usage	10
4.1	Running the program	10
4.2	OOFEM input file	13
4.3	Running finite element simulation in OOFEM	14
4.4	Post-processing	14
5	Comparison against experimental data and other applications	16
	References	21

1 Introduction and general information

Program Malcolm is a user-friendly parametric pre-processor for nonlinear analysis of concrete columns with multi-spiral reinforcement subjected to a combination of compression and bending. The program creates an input file for the finite element package OOFEM [9, 10, 11]. As shown later, to find an optimum configuration of multi-spiral reinforcement is not a trivial problem. The related experiments are very costly and time-demanding and show considerable scatter which makes the problem even more complicated. The search for the optimum configuration of the multi-spiral reinforcement can be accelerated if the nonlinear finite element (FE) simulations are embedded into the design process. The FE simulations are inexpensive and can examine structural response to an arbitrary loading path, and, after proper calibration of material parameters based on the experimental data the FE results can be used for the objective assessment the design performance.

Program OOFEM is computationally very efficient and easily extensible, yet it lacks any graphical user interface. The current version of the source files can be obtained at [OOFEM github repository](#) and then compiled. The next release (version 2.6) containing the updated material model as well as its extended documentation is expected in 2020.

Program Malcolm version 1.0 is written in Matlab syntax and was tested with version Matlab R2017a. The first version of the program can be treated as a development version. The feedback from the users will be incorporated into the software in 2020. As shown in the last section, the program has been successfully applied in a preliminary study to identify the key ingredients of the optimum design of axially compressed member with multi-spiral reinforcement.

1.1 Multi-spiral reinforcement

The concept of multi-spiral reinforcement for concrete columns introduced in 2005 by Samuel Yin [13], see Fig. 1 offers almost arbitrary shape of the cross-section but more importantly superior structural performance and more efficiently utilized potential of both materials, reinforcement and concrete.

In the case of circular columns reinforced with a single spiral, high ductility and improved strength is limited to compressive loading with a small eccentricity only. Whereas with the multi-spiral reinforcement (Fig. 2), superb structural performance and high resilience is obtained for almost arbitrary loading, which makes this solution suitable particularly for structures built in seismic regions.

As demonstrated in Figure 3 the multi-spiral layout of transverse reinforcement offers significantly better carrying capacity than conventionally reinforced columns with stirrups and ties. The Figure shows experimentally measured [8] strength of all 17 specimens plotted against the volumetric ratio of lateral reinforcement. Square symbols denote strength of the reference conventionally reinforced columns. Different colors mark specimens with the same diameter d_s of the small spirals. Filled and empty symbols distinguish stronger

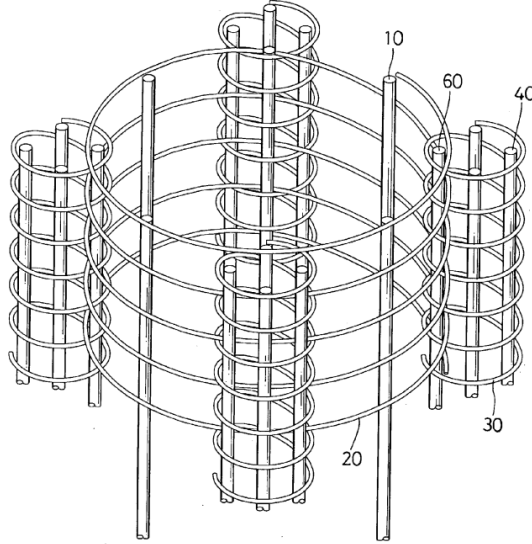


Figure 1: Multi-spiral reinforcement layout in the original U.S. patent of Samuel Yin [13].

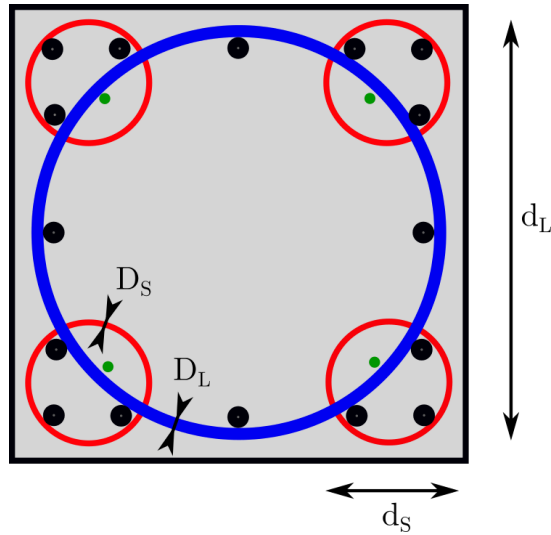


Figure 2: Reinforcement layout denoted as 5S4 for columns with multi-spiral reinforcement.

and weaker concrete grades, respectively, and the symbol size indicates the height of the pitch. From the data it is evident that the innovative multispiral reinforcement is superior to the conventional type, this difference which originates from the passively confined concrete is more pronounced in the case of stronger concrete and almost always exceeds 10 MPa. Owing to the experimental scatter (only 1 specimen tested for each configuration), it is next to impossible to infer and quantify any direct relationship between the reinforcement layout and the measured strength and thus to identify the ingredients of the optimum design. From Figure 3 it is evident that to find an optimum design of the

multi-spiral layout is not a trivial problem. The load carrying capacity is not simply a function of the lateral reinforcement ratio as could be expected. The level of lateral confinement which provides concrete with increased strength and ductility is linearly linked to the amount of reinforcing steel but also to the curvature of the spirals. Additional increase in confinement is produced in the overlapping regions of spirals where concrete becomes *double-confined* [14]. Higher number of spirals requires additional longitudinal reinforcement to produce a stiff reinforcement cage.

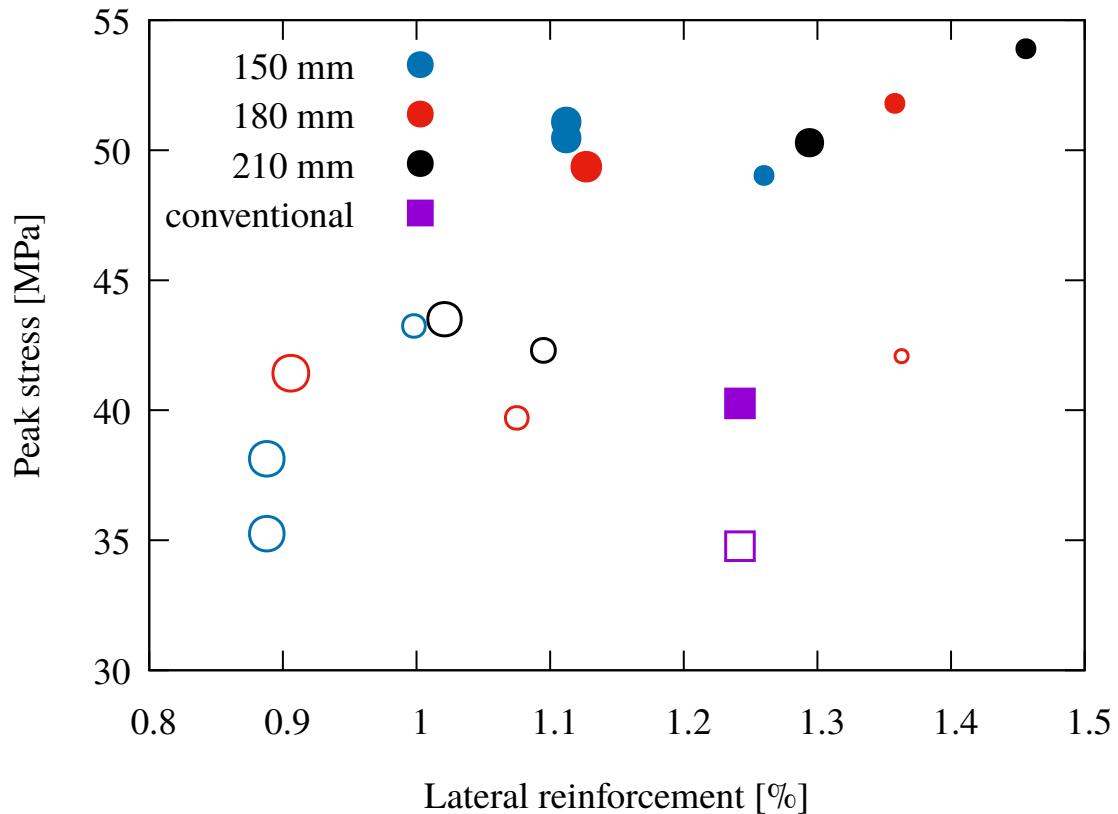


Figure 3: Dependence of the peak stress on the volume of lateral reinforcement in Kuo's experiment [8]. Filled and empty symbols correspond to stronger and weaker concrete, respectively, size indicates the height of the pitch. Colors distinguish specimens with the same d_s or with conventional reinforcement (purple).

2 Computational model

This section provides a brief overview of the computational models which are generated using program Malcolm.

The mesh of the finite element model combines a structured mesh for concrete (linear hexahedral elements) with regularly and irregularly discretized longitudinal and spiral reinforcement (truss elements), respectively. Finite element discretization of the concrete column is the same in both horizontal directions. The limit on maximum aspect ratio is 2. The hanging nodes are automatically generated at the intersections of the spirals with the volume finite element mesh. If the finite element mesh for concrete is too coarse, the discretization of the spirals is refined to better capture the geometry.

The two meshes are interconnected using the concept of hanging nodes, and the bond between concrete and steel is treated as rigid. The disabled slip is justified by the assumption that the tensile force in the steel spirals should be almost uniform over the length.

Provided that the failure mode is not localised, the full computational model of the entire column can be advantageously replaced with its representative section equal to the height of one pitch [5]. This reduction enables to introduce significantly denser finite element mesh which can help to thoroughly investigate the differences among different reinforcement alternatives. The effect of the boundaries is diminished by prescribing periodic boundary conditions on the top and bottom surfaces enabling them to freely warp. This also helps to eliminate the problem how to suitably choose the boundary conditions representing the connection between the column and the loading plates.

The program allows to select among different loading modes (currently only compression and/or bending) and different types of supports which are described in more detail in Section 4. The generated input file can be solved using the open-source finite element package OOFEM and the analysis is driven by a direct or indirect displacement control with the initial (elastic) stiffness matrix. If the computational model is large, it is recommended to switch from direct solver to an iterative solver which has considerably lower requirements on memory.

3 Material models

3.1 CDPM2

The behavior of concrete is described using the CDPM2 model (Con2DPM in OOFEM), proposed in 2013 by Grassl and coworkers [4]. The model is based on plasticity with isotropic hardening and non-associated flow [3], combined with a scalar damage model with damage driven by plastic flow and by the elastic strain. The yield condition is formulated in the effective stress space and depends on all three stress invariants. The flow rule is derived from a plastic potential that depends only on the hydrostatic stress and the second deviatoric invariant.

The model deals with the effective stress

$$\bar{\boldsymbol{\sigma}} = \mathbf{D}_e(\boldsymbol{\varepsilon} - \boldsymbol{\varepsilon}_p) \quad (1)$$

which is computed using the plastic part of the model. Here, \mathbf{D}_e is the elastic material stiffness matrix, $\boldsymbol{\varepsilon}$ is the total strain and $\boldsymbol{\varepsilon}_p$ is the plastic strain.

Afterwards, the effective stress is split into the positive part, $\langle \bar{\boldsymbol{\sigma}} \rangle_+$, and the negative part, $\langle \bar{\boldsymbol{\sigma}} \rangle_-$, and then reduced to the nominal stress as

$$\boldsymbol{\sigma} = (1 - \omega_t)\langle \bar{\boldsymbol{\sigma}} \rangle_+ + (1 - \omega_c)\langle \bar{\boldsymbol{\sigma}} \rangle_- \quad (2)$$

in which ω_t and ω_c are two independent damage variables for tension and compression, respectively.

To prevent mesh-dependent results, the model is in the present study regularized by a crack-band approach [1] (adjustment of a parameter that controls damage propagation depending on the finite element size). In tension, the softening curve which is derived from a cohesive traction-separation law of a bilinear type is used.

The constitutive model uses a large number of parameters which are summarized in Table 1. For more information please refer to the original paper [4] or to the updated documentation (matlibmanual) available at [OOFEM github repository](#).

In [4] it was recommended to adjust only a few basic parameters, most of which have a clear physical meaning, and to set all remaining parameters to their default values. Such recommendation is adopted also here except for the value of A_S which was identified from the slope of the post-peak descending branch.

3.1.1 Estimation of physically-based material parameters

The value of Young's modulus, uniaxial tensile strength, and fracture energy are derived from the mean compressive strength f_{cm} [MPa] (measured on cylinders at the age of 28 days) using the *fib* recommendations Model Code 2010 [2]. Once this value is specified by the user, the recommended values are computed using the following expressions.

The value of the initial modulus in GPa can be estimated using

$$E_{ci} = 21.5 (0.1 f_{cm})^{1/3} \quad (3)$$

The value of the mean tensile strength is computed differently for lower and stronger concrete grades

$$f_{ctm} = 2.12 \ln(1 + 0.1f_{cm}) \dots \text{for } f_{cm} \geq 58 \text{ MPa} \quad (4)$$

$$f_{ctm} = 0.3(f_{cm} - 8)^{2/3} \dots \text{for } 20 \leq f_{cm} \leq 58 \text{ MPa} \quad (5)$$

The value of fracture energy is computed accordingly to section 5.1.5.2 in MC 2010.

$$G_F = 73(f_{cm})^{0.18} \quad (6)$$

in this equation G_F is in N/m and the compressive strength is in MPa. The model CDPM2 deals with the crack opening instead of the fracture energy. For the case of bilinear softening (present case) the value can be computed from

$$w_f = 4.444 G_F / f_{ctm} \times 10^{-6} \quad (7)$$

The values of other parameters can be either adopted from CDPM2 paper or can be determined employing advanced identification techniques implemented in software [Identification of material model parameters for concrete](#) [7] which was also developed at CTU within CeSTaR project. This software combines the *fib* recommendations with the default values of the advanced parameters.

Table 1: Summary of parameters of CDPM2. Note that the values default for OOFEM might differ from the default values in Malcolm (e.g. H_p).

parameter	OOFEM identifier	unit	default value	meaning
E	E	Pa		Young's modulus
ν	n	-		Poisson's ratio
f_t	ft	Pa		uniaxial tensile strength
f_c	fc	Pa		uniaxial compression strength
w_f	wf	m		critical crack opening
e	ecc	-	0.525	eccentricity
q_{h0}	kinit	-	0.3	initial value of hardening variable q_{h1}
H_p	hp	-	0.5	hardening modulus (for the last stage)
D_f	dilation	-	0.85	dilation factor
A_h	Ahard	-	0.08	hardening parameter
B_h	Bhard	-	0.003	hardening parameter)
C_h	Chard	-	2	hardening parameter
D_h	Dhard	-	10^{-6}	hardening parameter
A_s	Asoft	-	15	softening parameter
ε_{fc}	efc	-	10^{-4}	softening parameter for compression
	stype		1	type of softening (1=bilinear)
w_{f1}/w_f	wf1	-	0.15	softening parameter for tension
σ_1/f_t	ft1	-	0.3	softening parameter for tension

3.2 Plasticity model for reinforcement

Currently, the most suitable material model for steel reinforcement in OOFEM is the Mises plasticity model with isotropic damage denoted as "MisesMat". The model uses the Mises yield condition (in terms of the second deviatoric invariant, J_2), associated flow rule, linear isotropic hardening driven by the cumulative plastic strain, and isotropic damage, also driven by the cumulative plastic strain.

The total strain is split into elastic and plastic parts

$$\varepsilon = \varepsilon_e + \varepsilon_p, \quad (8)$$

and the stress strain law reads

$$\sigma = (1 - \omega)\bar{\sigma} = (1 - \omega)\mathbf{D}(\varepsilon - \varepsilon_p), \quad (9)$$

in which $\bar{\sigma}$ is the effective stress, σ is the nominal stress, ω is the damage variable and \mathbf{D} is the elastic stiffness matrix.

The yield function is defined in terms of the effective stress

$$f(\bar{\sigma}, \kappa) = \sqrt{3J_2(\bar{\sigma})} - \sigma_Y(\kappa), \quad (10)$$

and the evolution of yield stress is captured by the linear hardening law

$$\sigma_Y(\kappa) = \sigma_0 + H\kappa, \quad (11)$$

in which the cumulative plastic strain is computed incrementally from the plastic strain increment.

$$\dot{\kappa} = \|\dot{\varepsilon}_p\|, \quad (12)$$

Finally, the evolution laws for the plastic strain and damage read

$$\dot{\varepsilon}_p = \dot{\lambda} \frac{\partial f}{\partial \bar{\sigma}}, \quad (13)$$

$$\dot{\omega}(\kappa) = \omega_c(1 - e^{-a\kappa}), \quad (14)$$

This model can be calibrated to provide both simplified code-like bilinear stress-strain relationship as well as realistic experimental response.

4 Usage

4.1 Running the program

A sequence of 8 dialogues guide the user through the specification of the dimensions, finite element mesh density, reinforcement topology, material properties, and finally the boundary conditions. In the end the topology of the computational model can be visualized. This section provides a brief explanation of the procedure.

1. Square column geometry

Only a square cross-section of the column is supported. The user is asked to provide the width and height of the column in meters. Experience indicates [5] that the full model can be advantageously replaced by a representative section with height equal to the spiral pitch. This significant reduction in computational cost allows to use finer element mesh necessary to correctly capture the complex stress distribution in the overlapping regions and in the corners of the column. The default dimensions are $0.6 \times 0.6 \times 0.075$ m which corresponds to a representative section of Y8 specimen in Kuo's study [8].

2. Finite element size

The program generates structured and uniform finite elements mesh composed of brick elements with linear approximation of displacements. Default element size origins from 15 elements in horizontal direction (same division in both lateral directions) which already provides a reasonable accuracy, 4 elements in vertical direction and the aspect ratio. The aspect ratio is automatically checked and the maximum allowed value is 2:1. The predefined values can be arbitrarily changed but if the aspect ratio is exceeded, the finite element size is adjusted accordingly.

3. Reinforcement topology

The program supports only 5S4 reinforcement layout (see Figure 2) with one central spiral and 4 smaller spirals in the corners of the cross-section. The outer diameter of the large spiral is fully defined by the column width and the concrete cover because the goal is to minimize the area of unconfined concrete. The thickness of the concrete cover can be modified and its default value is 25 mm. The second parameter is the spiral pitch. This property is uniform for all spirals and is defined as a distance center-to-center. If the column height is less or equal than 100 mm, the pitch is set equal to this height because it is anticipated that the representative segment of the column is being modelled. For larger height the default pitch value is 75 mm. Pitch height is automatically decreased to yield an integer number of spiral loops. It is the user's responsibility to provide a reasonable value of the small spiral outer diameter. The topology of vertical bars is defined automatically.

4. Reinforcement specification

Next, the diameter and the steel quality is assigned to small spirals, large spiral and

vertical rebars. The scale is imperial. Table 2 shows (approximately) equivalent metric sizes and the net cross-sectional areas. For the three types of reinforcement the user can choose from the steel grades listed in Table 3. This stiffness is in all cases 200 GPa. The yield stress f_y is specified in the second column of the table.

The last three columns in the Table show the parameters of the Mises plasticity model with hardening and damage. The parameters were adjusted to give the values of tensile strength f_u and the strain at peak stress ε_{peak} . Properties of the SD420 steel are taken from the Kuo's experiment [8]. The last line is the ideally elasto-plastic material model without hardening and without any strain limit.

imperial [1/8 in]	metric [mm]	area [mm ²]
#3	10	71
#4	13	129
#5	16	200
#6	19	284
#7	22	387
#8	25	509
#9	29	645
#10	32	819

Table 2: Imperial system of reinforcing bars

designation	f_y [MPa]	f_u [MPa]	ε_{peak} [%]	H [GPa]	ω_c [-]	a [-]
SD420	473	668	10	7.5	1	6
SD420	479	723	10	8.2	1	6
B500A	500	525	2.5	9	1	13
B500B	500	540	5.0	5.5	1	7.25
B500C	500	575	7.5	5.5	1	6.15
B500	500	500	∞	0.	0	0

Table 3: Material characteristics of reinforcing bars and material parameters of Mises material with hardening and damage.

5. Concrete compressive strength f_{cm} [MPa]

Mean value of the uniaxial compressive strength measured on cylinders is the basic parameter from which the stiffness and tensile properties of concrete are determined using *fib* Model Code 2010. It is generally accepted that the mean strength is equal to the characteristic strength increased by 8 MPa and so the default value $f_{cm} = 38$ MPa corresponds to concrete class C30/37.

6. CDPM2 Parameters

The values of the advanced material parameters of CDPM2 can be either taken by their default values or the newly developed identification software can be used for

their determination if the related experimental data are available. The complete list of material parameters of CDPM2 is summarized in Table 1.

7. Boundary conditions

It is possible to choose among three different types of supports:

- **Fully fixed** supports restrain all degrees of freedom at the base of the column. The lateral displacement of the top surface is linked to the bottom surface and thus is also constrained.
- **Vertically fixed** supports restrain only vertical degree of freedom but allow free lateral expansion or contraction of the column's end. This condition also prescribes that the top surface will remain plane after deformation.
- **Periodic BC** (default) enables modeling representative segments of the columns. The degrees of freedom on the top and the bottom surface of such segment are linearly constrained. This condition does not disable warping as in the preceding case.

One of four different loading scenarios can be chosen:

- **Axial compression** (direct displacement control), default. Linearly increasing vertical displacement is prescribed to all nodes on the top surface. The top and bottom surfaces remain parallel after deformation (but can warp if periodic BC is selected). The end of simulation corresponds to total shortening of 3%, the reference value of displacement imposed by the boundary condition is 1%.
- **Eccentric compression** (indirect displacement control). Load level is related to 1 MN compressive force acting at arbitrary location of the top surface which is specified by dimensionless coordinates x_F/B [-] and y_F/B [-]. The corners of the cross-section correspond to value 0.5. Default values are 1/6 and 0, respectively, which (according to the beam theory) results in completely compressed cross-section and the neutral axis coinciding with the opposite side of the cross-section. Periodic boundary conditions are not supported.
- **Pure bending** (direct displacement control) prescribes a fixed ratio of monotonically increasing curvature with respect to both axes. In the following dialog, unity corresponds to curvature 0.01 m^{-1} . Default values are $\kappa_{a1} = 1$ and $\kappa_{a2} = 0$. Displacement in the axial direction of the column is not prevented.
- **Compression and bending** (direct displacement control) prescribes additional constraint in the longitudinal direction. The default proportions of loading are $\varepsilon : \kappa_1 : \kappa_2 = 1 : 0.2 : 0$.

Please note that loading in shear is not supported. However, it can be prescribed manually by editing the input file accordingly.

8. Plot

The geometry of the column, the outline of the finite element mesh and the topology of the reinforcement can be visualized. This serves as a good check. The result obtained with completely default settings is shown in Figure 4.

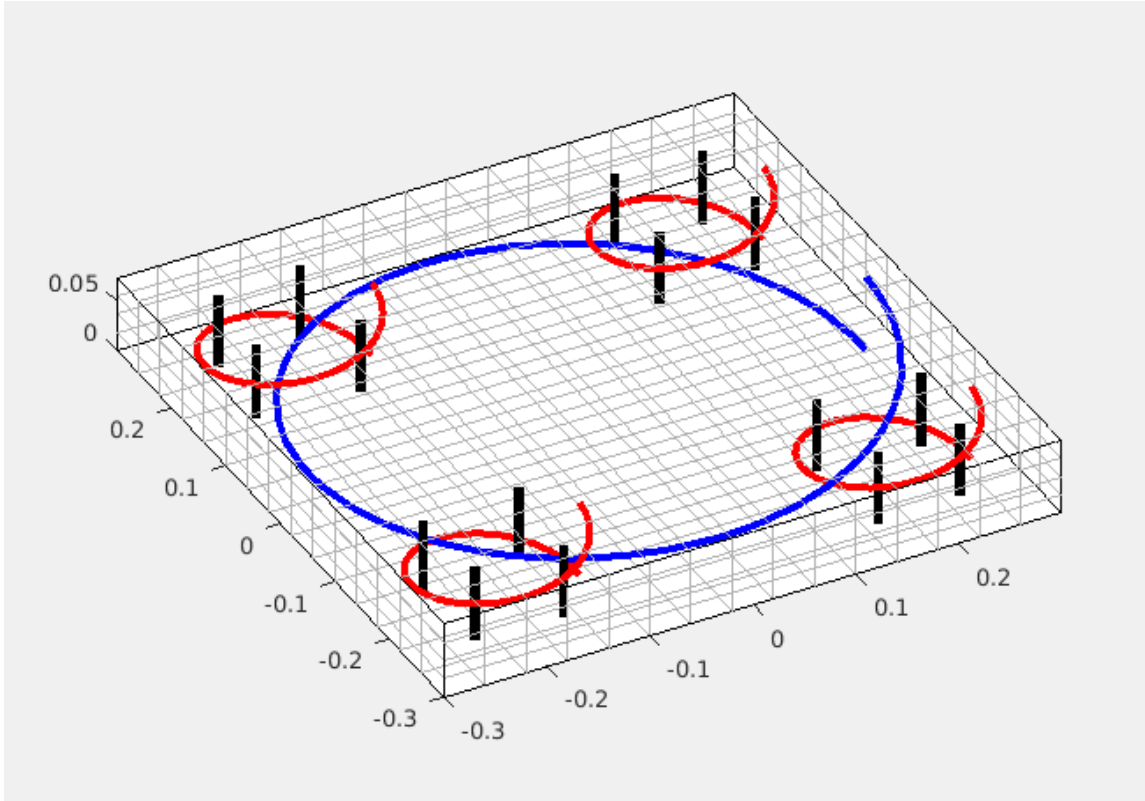


Figure 4: Segment of a square column $600 \times 600 \times 75$ mm with prescribed periodic boundary conditions. This model can be obtained with default settings.

4.2 OOFEM input file

The generated input file can be immediately processed by the FE package OOFEM. No modifications are necessary but are possible. The conventions of the OOFEM input file are described in detail in [OOFEM input data format specification](#). The following list provides additional explanation which might be useful.

- Header section contains user-defined column dimensions, concrete cover, and the reinforcement specification: pitch H , d_s , D_L , D_S , D_V
- Header section shows the reinforcement ratio in vertical and horizontal direction in %
- The analysis setup can be modified by adjusting: `rtolv`, `nsteps`, and solver properties. Large problems should be computed using iterative solvers, to activate it use

```
smtype 4 and lstype 1 lstol 1e-4 lsiter 1000 lsprecond 4
```

- To modify graphical export in vtu standard modify `vtkxml` definition (most important variables and the frequency of export, default value is every 5th step)
- In the case of indirect control (eccentric compression) it is possible to modify the position of the loading force. The position corresponds to the topology of the last hanging node.
- The cross-sections of truss elements can be modified to reflect different reinforcement area (2 = large spiral, 3 = small spiral, 4 = vertical rebars).
- The material models and their parameters can be modified. The following numbers are defined: 1 = concrete, 2 = large spiral, 3 = small spiral, 4 = vertical rebars.
- The following numbering convention is used for the boundary conditions:
 - 1 = fixed displacement
 - 2 = shortening, value corresponds to 1% overall shortening
 - 3 = curvature, value corresponds to curvature $\kappa_y = 0.01 \text{ m}^{-1}$ - axes correspond to the global coordinate system not to beam convention.
 - 4 = curvature, value corresponds to curvature $\kappa_x = 0.01 \text{ m}^{-1}$
 - 5 = 1 MN load used as a reference in the case of indirect control
- The time functions should be modified and extended to reflect more complex loading history. The number of each time function corresponds to the number of the boundary condition.

4.3 Running finite element simulation in OOFEM

Once the OOFEM input file has been generated by Malcolm, it can be (after possible necessary adjustments) computed with OOFEM finite element solver. The executable of the OOFEM solver can be either downloaded directly from the [OOFEM web page](#), or it can be compiled from the source files, please refer to the [OOFEM git tutorial](#) for more information.

The analysis is started by running the command (in terminal/command line)

```
$ path_to_oofem_executable -f oofem_input_file.in.
```

Please refer to [OOFEM manuals](#) for more information.

4.4 Post-processing

The computed results can be either visualized using any vtk-standard supporting post-processor, e.g. (free and open-source) [Paraview](#) [6]. The graphical results are stored separately for concrete, spiral reinforcement and longitudinal reinforcement. By default,

the graphical results are generated for every 5th step. For concrete the following quantities can be visualized:

- strain tensor (id 1)
- stress tensor (id 4)
- damage tensor (id 13)
- plastic strain tensor (id 27)

and for reinforcement

- stress tensor (id 1)
- strain tensor (id 4)
- plastic strain tensor (id 27)

If needed, more variables can be added into the vtkxml export module. Please refer to `oofem/src/oofemlib/` for the code number.

It is worth mentioning that the first component (0th in Paraview) of the damage tensor corresponds to tensile damage, 2nd (4th in Paraview) to compressive damage, and 3th (8th in Paraview) to dissipated work density. Also note that in the case of reinforcement the stresses and strains are shown with respect to local coordinate system, i.e. σ_x (component 0 in Paraview) corresponds to the axis of the truss elements and not stress in direction of the global axis x .

The global response can be very conveniently assessed by observing the stress-strain (or force-displacement) curve. The data for this curve can be gathered using parser called extractor. This program can be found at `oofem/tools`. To use it and to store the results to an arbitrary text file run

```
$ python extractor -f oofem_input_file.in >> name_of_the_text-file. It is very convenient to use (free and open-source) program Gnuplot [12] for the graphical output.
```

5 Comparison against experimental data and other applications

The experimental data on monotonic loading of concrete columns with multi-spiral reinforcement in compression are scarce.

In the present example the model parameters were calibrated based on the standard laboratory data and the response of a representative large-scale specimen labeled "Y8" in Kuo [8] ($H = 75$ mm, $d_S = 180$ mm, #3 for D_S and #4 for D_L). The calibrated material model was then used for prediction of structural behavior for various configurations of reinforcement.

Parameter identification started with a separate calibration of the extended Mises model based on the experimental data for steel. For the longitudinal reinforcement the yield strength was set to 497 MPa, parameters controlling the hardening and damage law were adjusted to yield the peak stress 723 MPa at strain 10%. Similarly, for the transverse reinforcement (average strengths of #3, #4, #5 rebars) the corresponding values were 473 and 668 MPa.

For concrete (CDPM2), the value of its uniaxial compressive strength was initially set to the *specified* strength, $f'_c = 34.3$ MPa and the remaining parameters were set as described in the previous section. However, the carrying capacity was substantially overestimated. To get a reasonable agreement, the compressive strength had to be decreased to 28 MPa. This might be explained by different quality of concrete in the standard laboratory experiments and in the large-scale experiments. According to *fib* recommendations, the Young's modulus was set to $E = 30.3$ GPa, Poisson's ratio $\nu = 0.2$, uniaxial tensile strength $f_t = 2.21$ MPa, fracture energy $G_f = 133$ N/m, and finally, by a trial-and-error procedure, $A_S = 15$. Also note that the experimental data has been processed to yield a reasonable stiffness, the initial original loading path in the load-displacement diagram corresponded to stiffness of only ≈ 5 GPa. This is probably caused by the readings from the loading machine instead of external sensors.

The response is shown in Figure 5 for the standard mesh ($45 \times 45 \times 7$ elements), $2\times$ refined ($90 \times 90 \times 15$ elements), and $2\times$ coarser meshes ($20 \times 20 \times 3$ elements). Despite huge differences in computational time and local stress and damage distribution, the overall response is very similar.

In the present case, the potential layout of the reinforcement is described by four variables only, D_S , D_L , d_S , see Fig.2, and the pitch of the spiral H . The diameter of the reinforcing bars corresponded to the imperial rebar scale from #3 (approx D10) to #7 (approx D22), the outer diameter of the small spiral ranged from 120 mm to 260 mm with 10 mm step, and three different values of the spiral pitch, 55 mm, 75 mm, and 95 mm were investigated. This produces a set of 1125 combinations with the overall reinforcement ratio from 0.64% to 9.39%. In order to investigate a reasonable set that we will be able to compute by brute force method, this range was narrowed only to those alternatives with the reinforcement ratio from 1.1% to 2.9% which yielded 476 combinations. With the average computational time of 2 days (3.2 GHz CPU) for one analysis, the total

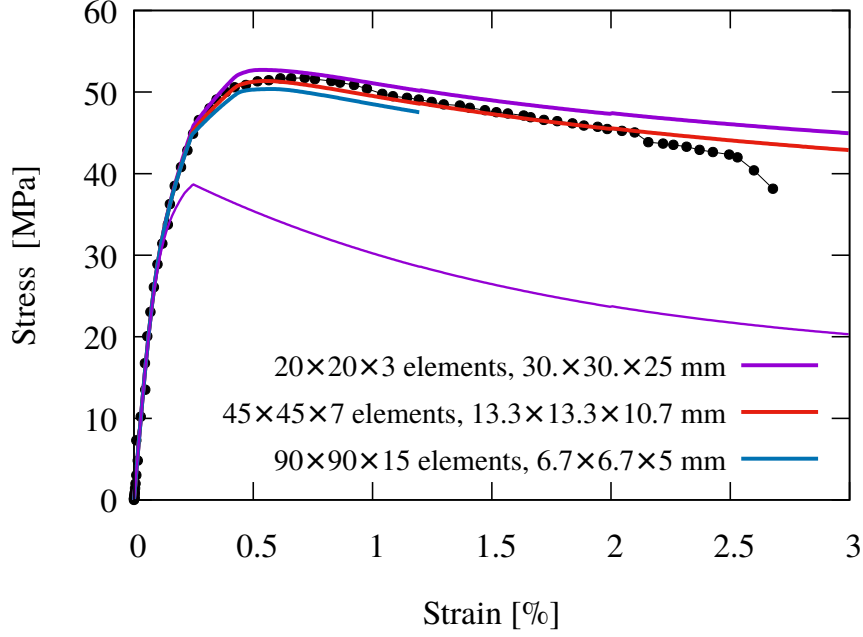


Figure 5: Calibration of the computational model to match the experimental data of Kuo's [8], Y8 specimen. Thick solid lines indicate the results of the FEM simulation with different notional size of the FE and the thin line denotes the solution without transverse reinforcement.

computational time exceeded 16 days on a computer with 60 cores.

The simulation of a displacement-driven uniaxial compression test has been done for each combination of the transverse reinforcement and run on a representative section of the column. The values of the peak load which were automatically extracted from the non-linear load-displacement curves at the end of each simulation. In order to provide a better comparison and to show the increase in carrying capacity, the peak load is divided by the cross-sectional area of the column and is presented in terms strength. Note that this strength comprises the contribution of the longitudinal reinforcement which contributes by 10.7 MPa (only approximately since the stress-strain law is hardening and the peak strength was reached at different value of axial strain for each combination).

An overall summary of the results is presented in Fig.6 in which the strength is plotted against the ratio of transverse reinforcement for each combination. In this Figure, the Pareto front which corresponds to the solutions with the best strength vs. reinforcement performance is shown in red filled circles, and the remaining alternatives in blue empty circles. In the investigated range, the Pareto front forms a slightly nonlinear concave shape which can be with a reasonable accuracy approximated by a linear function with a slope of 10.8 MPa per 1% of transverse reinforcement. The intercept with the vertical axis (at 0%) is at 37 MPa which is only 1.7 MPa less than the value of average strength obtained from a simulation without lateral reinforcement (and thus without multi-axial

stress state and related strength increase due to lateral confinement).

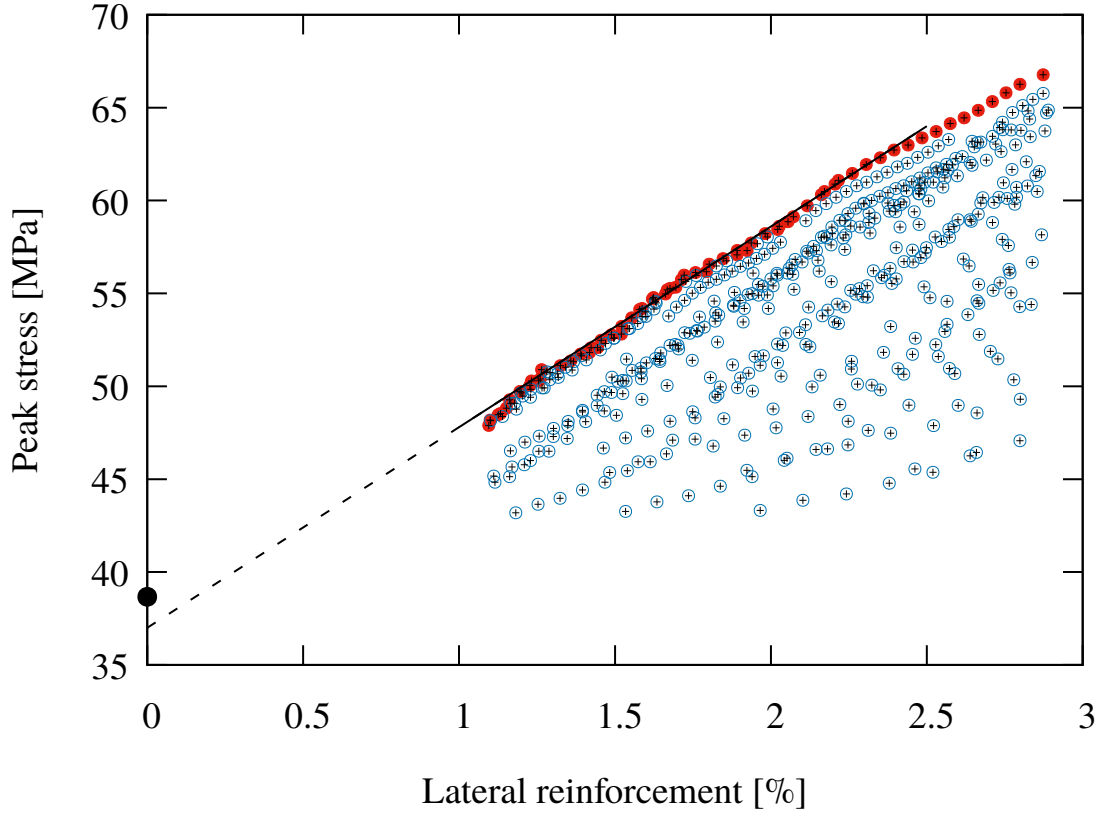


Figure 6: Dependence of peak stress on ratio of transverse reinforcement for different configurations of reinforcement. The Pareto front and its linear approximation are shown in red color and solid black line, respectively.

As expected, the performance drops with increasing pitch, as illustrated in Figure 7, where different colors are used for the model with 55, 75 and 95 mm height. With increasing height the stress transfer of the confining action becomes less effective and the size of the confined region shrinks which in turn results into decrease in strength. This influence becomes more pronounced with increasing reinforcement ratio (approx. above 1.7%).

The results of the finite element analysis suggest that perhaps the most important factor which influences the efficiency of the lateral reinforcement (with respect to strength in uniaxial compression) is the balance between the confinement stress (computed by a simple expression assuming on uniform stress inside the spiral) produced by the large and small spiral, $\sigma_{lat,L}$, $\sigma_{lat,S}$, respectively. The ratio $\sigma_{lat,L}/\sigma_{lat,S}$ is reflected by the size of a circle in Figure 8. In the Figure it is evident that for $\sigma_{lat,L}/\sigma_{lat,S} \geq 1$ the solution lies close to the Pareto front if not in it.

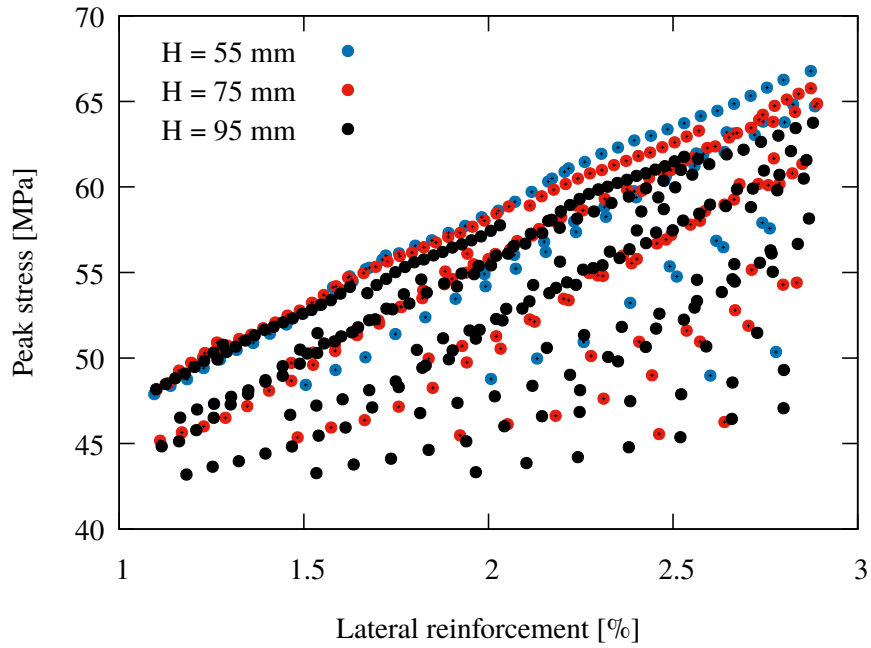


Figure 7: Influence of the spiral pitch on the strength vs. transverse reinforcement ratio.

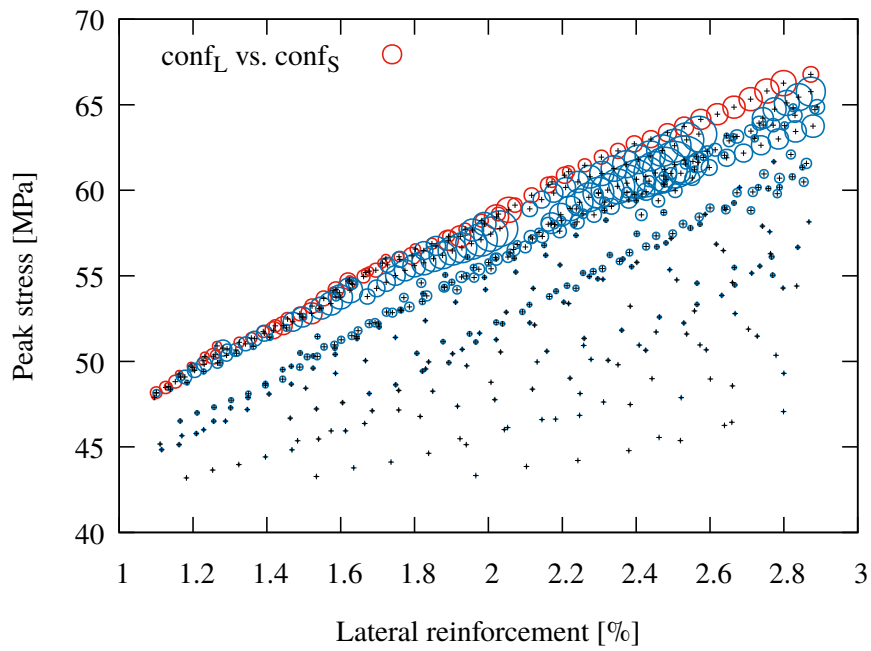


Figure 8: Influence of the ratio of the lateral confinement produced by the large and small spiral on the strength vs. transverse reinforcement ratio. The size of the symbol in the legend corresponds to unity.

Acknowledgment

Financial support for this work was provided by the Technology Agency of the Czech Republic (TAČR), project number TF05000040 (CeSTaR: Computer simulation and experimental validation - complex service for flexible and efficient design of pre-cast concrete columns with innovative multi-spiral reinforcement).

References

- [1] Z. P. Bažant and B. H. Oh. Crack band theory for fracture of concrete. *Matériaux et Construction*, 16(3):155–177, May 1983.
- [2] Fédération Internationale du Béton. *Model Code 2010*. Number vol. 65 in fib Bulletin. International Federation for Structural Concrete (fib), 2012.
- [3] P. Grassl. Modelling of dilation of concrete and its effect in triaxial compression. *Finite Elements in Analysis and Design - FINITE ELEM ANAL DESIGN*, 40:1021–1033, 06 2004.
- [4] P. Grassl, D. Xenos, U. Nyström, R. Rempling, and K. Gylltoft. CDPM2: A damage-plasticity approach to modelling the failure of concrete. *International Journal of Solids and Structures*, 50(24):3805 – 3816, 2013.
- [5] P. Havlásek, M. Jirásek, and Z. Bittnar. Modeling of precast columns with innovative multi-spiral reinforcement. fib Proceedings, pages 2301–2307. FIB - Féd. Int. du Béton, 2019.
- [6] A. Henderson. *ParaView Guide, A Parallel Visualization Application*. Kitware Inc., 2007.
- [7] E. Janouchová, K. Mikeš, and A. Kučerová. Identification of material model parameters for concrete. http://mech.fsv.cvut.cz/~phavlasek/2018_cestar.php, 2019.
- [8] M. Kuo. *Axial Compression Tests and Optimization Study of 5-Spiral Rectangular RC Columns, Master Thesis (in Chinese)*. National Chiao Tung University, Hsinchu, Taiwan, 2008.
- [9] B. Patzák, , et al. Object Oriented Finite Element Method - OOFEM. <http://www.oofem.org>, since 1993.
- [10] B. Patzák. OOFEM home page. <http://www.oofem.org>, 2000.
- [11] B. Patzák. OOFEM - an object-oriented simulation tool for advanced modeling of materials and structures. *Acta Polytechnica*, 52(6):59–66, 2012.
- [12] T. Williams, C. Kelley, and many others. Gnuplot 4.6: an interactive plotting program. <http://gnuplot.sourceforge.net/>, April 2013.
- [13] S. Yin. Helical rebar structure, 2005. US Patent 6,860,077.
- [14] S. Y.-L. Yin, T.-L. Wu, T. C. Liu, S. A. Sheikh, and R. Wang. Interlocking spiral confinement for rectangular columns. *Concrete International*, 33(12), 2011.